Effects of Ionic Liquids on Enzymatic Catalysis of the Glucose Oxidase toward the Oxidation of Glucose

Xiuming Wu, Bo Zhao, Ping Wu, Hui Zhang,* and Chenxin Cai*

Jiangsu Key Laboratory of Biofunctional Materials, College of Chemistry and Environmental Science, Nanjing Normal University, Nanjing 210097, P. R. China

Received: June 16, 2009; Revised Manuscript Received: August 21, 2009

The effects of ionic liquids (ILs) on the catalytic activity of enzymes were studied by approaches of electrochemistry and quantum chemistry calculation in this work. Three types of ILs, namely, [bmpyri]BF_4, [bmpyrro]BF_4, and [bmim]BF_4, were selected to address the effects of different types of ILs on the electrocatalytic activity of glucose oxidase (GOx) toward the oxidation of glucose. ILs and GOx were assembled on the surface of an electrode via single-walled carbon nanotubes (SWNTs) and poly(sodium 4-styrenesulfonate) (PSS) utilizing the electrostatic interaction. Spectroscopic results indicated that ILs did not affect the conformation of the enzyme. The cyclic voltammetric results showed that the electrocatalytic activity of the GOx−IL−PSS−SWNTs/GC electrode was lower than that of the GOx−SWNTs/GC electrode. The characteristic kinetic constants of the enzymatic reaction were evaluated from the cyclic voltammograms under a substrate-saturated condition. The values of the characteristic rate constant obtained at each IL-containing enzyme electrode were lower than those obtained at the GOx−SWNTs/GC electrode and decreased following the sequence of SWNTs > [bmpyri] > [bmpyrro] > [bmim]. The theoretical calculations combined with experiments were employed to address the interaction between the ILs and SWNTs, showing that the presence of IL on the surface of SWNTs could significantly affect the electrical transfer properties of the nanotube and led to the decrease of the electrocatalytic activity of the GOx−IL−PSS−SWNTs/GC electrode. These results indicate that the nature of ILs is the main factor, which affects the electrocatalytic activity of the GOx−IL−PSS−SWNTs/GC electrodes toward the oxidation of glucose. The results of this study are directly relevant for those applications where ILs are employed in the form of thin films supported on solid surfaces, such as the designing of the related biosensor, microelectronic devices in the ILs-containing system, and so forth.

1. Introduction

Ionic liquids (ILs), which are composed solely of an organic cation and an organic or inorganic anion, have been exploited for use in various fields,[1−11] including in electrochemistry, synthetic chemistry, catalysis, polymerization, and so forth. In particular, the application of ILs in the area of electrochemistry has received tremendous attention in the past few years.[3,12−16] For example, ILs have already been shown to offer advantages in electrochemical studies when used as either the solvent or electrolyte or both. The wide potential window (5−6 V)[3,13] makes it possible to electrodeposit various metals at potentials that cannot be obtained in aqueous electrolyte solutions.[17] The high ionic conductive nature of ILs eliminates the need for supporting electrolyte, simplifying the electrochemical measurements.[18] Specific capacitance, good stability, and wide potential window also make ILs attractive as electrolytes for capacitor applications.[19]

Recently, the application of ILs in the field of biocatalysis and biosensor fabrication has attracted considerable attention.[8,11,14,20−39] Compared with those observed in other organic solvents, enzymes in ILs have presented enhanced activity, stability, and selectivity as well as better recoverability and recyclability.[29,33−39] However, the results of these studies cannot be compared directly with each other because they were obtained under different conditions. Moreover, some contradicting results even existed.[23,25] In addition, though the complex interactions between ILs and proteins/enzymes have been studied, understanding is not yet complete and does not provide a basis for predicting the activity and stability of enzymes in ILs.

Considering these, we have conducted a systematic study on the effects of ILs on the electrochemical characteristics of heme-containing proteins/enzymes.[40] Our goal is to elucidate effects of ILs on the kinetics of enzymatic reaction and to predict the catalytic performance of enzyme in different types of ILs. In our recent work, we have investigated the oxidation of glucose catalyzed by glucose oxidase (GOx) under a substrate-saturated condition in the mixture of 1-butyl-3-methylimidazolium tetrafluoroborate ([bmim]BF_4) and phosphate buffer solution (PBS).[41] The results demonstrated that the catalytic current decreased with the increase of the content of IL in buffer. The key factor of causing the decrease of the catalytic current is the reduction in the diffusion rate of the mediator and the substrate, which results from the increase in the solution viscosity after the addition of the IL. To further understand the effects of ILs on the catalytic activity of enzymes and to eliminate the effect of the solution viscosity on the catalytic current, in this work, we immobilized ILs and enzyme on the surface of electrode via SWNTs. The GOx is again chosen as a model for its stability, its ability to be immobilized on the electrode surface, and its electrical communication with the electrode surface.[42,43] Three types of ILs, namely, 1-butyl-3-methylpyridinium tetrafluoroborate ([bmpyri]BF_4), 1-butyl-1-methylpyrrolidinium

* Corresponding author. E-mail: zhangh@njnu.edu.cn; cxcai@njnu.edu.cn.

10.1021/jp905632k CCC: $40.75
Published on Web 09/11/2009

SCHEME 1: Schematic Illustration of the Processes of Immobilization of ILs and GOx on the Surface of SWNTs by Using Layer-by-Layer Deposition Taking Advantage of the Electrostatic Adsorption between SWNTs, PSS, ILs, and GOx

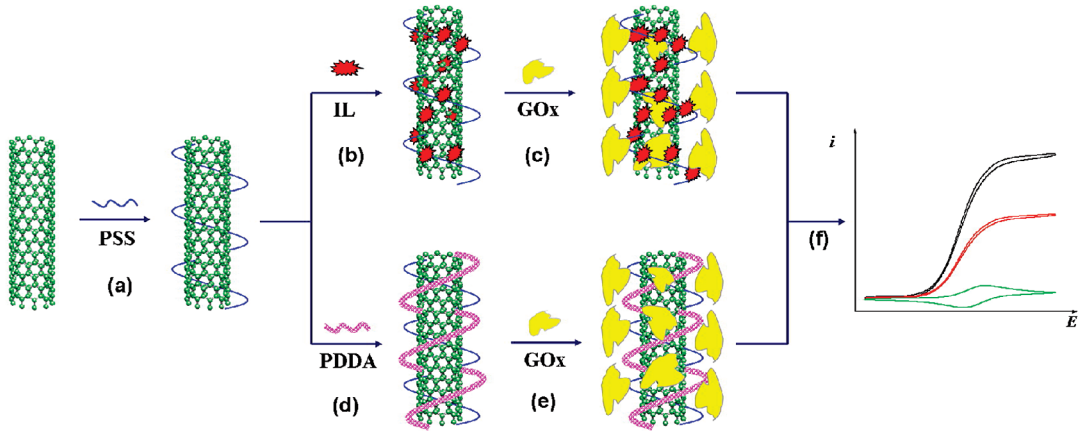

tetrafluoroborate ([bmpyrro]BF_4), and [bmim]BF_4, were selected to study the effects of different types of ILs on the catalytic system. The characteristic kinetic constants for the enzymatic reaction were evaluated by the use of cyclic voltammetry. The effects of ILs on these characteristic rate constants were discussed by approaches of electrochemistry and quantum chemistry calculation.

2. Experimental Section

2.1. Chemicals. GOx (EC 1.1.3.4, from *Aspergillus niger*, ~200 U/mg, Sigma), β-D-glucose (Sigma), [bmpyri]BF_4 (99%, Alfa Aesar), [bmpyrro]BF_4 (98%, Alfa Aesar), [bmim]BF_4 (98+%, Alfa Aesar), and ferrocenecarboxylic acid (FcA, 97%, Aldrich) were used as received. Poly(sodium 4-styrenesulfonate) (PSS, 30 wt % solution in water, MW ~70 000, Aldrich) and poly(dimethyldiallylammonium chloride) (PDDA, 20 wt % in water, MW 100 000−200 000, Aldrich) were diluted to 5% with water before use. SWNTs (<2 nm in diameter, Shenzhen Nanotech Port, Shenzhen, China) were treated following the procedures reported previously.[44] All other chemicals were of analytical grade. All solutions were prepared with double-distilled water. PBS (0.1 M, pH 8.2) was made up from Na_2HPO_4 and NaH_2PO_4. The glucose stock solution was allowed to mutarotate for at least 24 h before use.

2.2. Assembly of ILs and GOx on the Electrode Surface. ILs and GOx were assembled layer-by-layer on the surface of SWNTs by taking advantage of the electrostatic interaction of these components (SWNTs, PSS, ILs, and GOx) involved in the electrode fabrication. Several experimental parameters were optimized to obtain the best voltammetric response. Typically, 1 mg of SWNTs was dispersed in 1 mL of CTAB (cetyltrimethylammonium bromide) aqueous solution (1 wt %) with the aid of ultrasonication forming a 1 mg/mL SWNTs suspension. When SWNTs were sonicated and incubated in the solution, the CTAB molecules were adsorbed on the surface of SWNTs through hydrophobic interactions creating a distribution of positive charges on the SWNT surface. These charges prevent the SWNT aggregation and induce their suspension in water. Afterward, the CTAB-coated SWNTs were collected by centrifugation at 18 000 rpm for 30 min. The supernatant was removed, and the SWNTs (*hereafter, unless otherwise specified, the SWNTs are referred to CTAB-coated SWNTs*) were thoroughly washed at least thrice with water to remove the loosely adsorbed CTAB. To fabricate the SWNTs/GC electrode, 2 mg of SWNTs was dispersed in 1 mL of water to give a 2 mg/mL SWNT suspension. Then, 2 μL of the suspension was cast onto the surface of the pretreated glassy carbon electrode[38] (GC, 3 mm in diameter, CH Instruments) with a microsyringe, and the solvent (water) was allowed to evaporate at ambient temperature before use.

To assemble ILs and GOx on the surface of the SWNTs/GC electrode, the electrode was first immersed in PSS solution (5 wt %) for 30 min to obtain a negatively charged surface (step a, Scheme 1). The resulting PSS−SWNTs/GC electrode was thoroughly rinsed with water to remove the loosely adsorbed PSS. Then, the electrode was incubated in [bmim]BF_4 aqueous solution (1 mM) for 20 min resulting in the [bmim]−PSS−SWNTs/GC electrode (step b, Scheme 1). The surface charge of the [bmim]−PSS−SWNTs/GC electrode was turned to be positive due to the adsorption of the [bmim] cation. After rinsing with water, the electrode was used for assembling GOx by incubating it in GOx solution (5 mg/mL in PBS solution, pH 8.2) at 4 °C for 1 h (step c, Scheme 1). GOx is negatively charged in pH 8.2 PBS since the isoelectric point of the enzyme is ~4.2.[45] Therefore, the enzyme can be easily assembled on the surface of the [bmim]−PSS−SWNTs/GC electrode forming the GOx−[bmim]−PSS−SWNTs/GC electrode. After being thoroughly rinsed with water, the electrode was ready to be used for catalytic oxidation of glucose (step f, Scheme 1). The electrode was stored at 4 °C when not in use. The total amount of GOx (Γ_E, in mol) deposited on the electrode surface was estimated from the change of the concentration of GOx in solution before and after adsorption. The concentration of GOx was determined spectrophotometrically using an extinction coefficient of 1.41×10^4 M^{-1} cm^{-1} for GOx at 450 nm.[46] A molecular weight of about 186 000 g/mol for GOx was used for calculation.[46]

If [bmim]BF_4 was replaced by [bmpyri]BF_4 and [bmpyrro]-BF_4, respectively, at step b (Scheme 1), the GOx−[bmpyri]−PSS−SWNTs/GC and GOx−[bmpyrro]−PSS−SWNTs/GC electrode could be fabricated. To further study the effect of ILs on the oxidation of glucose catalyzed by GOx, the IL was also replaced by PDDA to immobilize GOx (steps d and e, Scheme 1). The resulting electrode was denoted as the GOx−PDDA−PSS−SWNTs/GC electrode.

2.3. Apparatus and Procedures. UV−vis absorption was measured at a Cary 5000 UV−vis−NIR spectrophotometer (Varian). The FTIR spectrum was recorded on a Nexus 670 FT−IR spectrophotometer (Nicolet Instruments) using a KBr disk at a resolution of 4 cm^{-1}. Circular dichroic (CD) measurements were made on a JASCO model J-810 dichrograph (Japan Spectroscopic Co. Ltd.) in a 1 cm quartz cuvette. The final

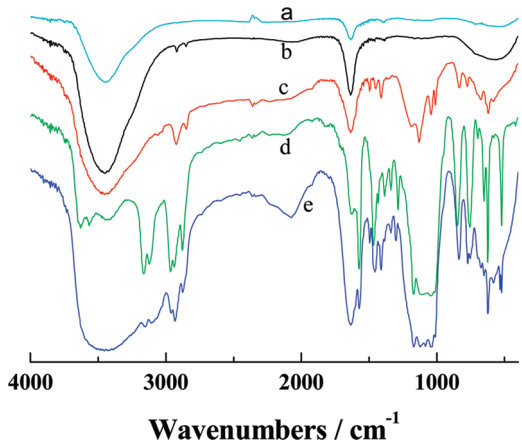

Figure 1. FTIR spectra of the SWNTs (a), SWNTs adsorbed with CTAB (b), SWNTs−PSS (c), [bmim]−PSS−SWNTs (d), and GOx−[bmim]−PSS−SWNTs (e).

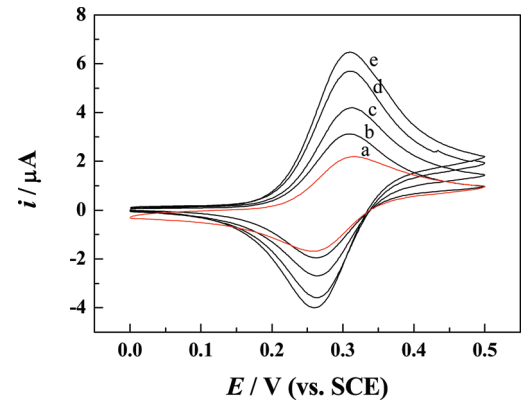

Figure 2. Cyclic voltammetric responses of 0.5 mM FcA in 0.1 M PBS (pH 8.2) at the bare GC (a), [bmim]−PSS−SWNTs/GC (b), [bmpyrro]−PSS−SWNTs/GC (c), [bmpyri]−PSS−SWNTs/GC (d), and SWNTs/GC electrode (e). The scan rate was 10 mV/s.

spectra were the mean of ten accumulated scans and were corrected for the unspecific dichroic absorbance of the medium.

The cyclic voltammetric experiments were performed with a CHI 660B electrochemical workstation (CH Instruments). A coiled Pt wire and a saturated calomel electrode (SCE) were used as the counter electrode and the reference electrode, respectively. The buffer (0.1 M PBS, pH 8.2) was purged with high-purity nitrogen for at least 30 min prior to each measurement, and a nitrogen environment was kept over solution to protect the solution from oxygen. All electrochemical experiments were performed at room temperature (22 ± 2 °C).

3. Results

3.1. Characterization of the Assembly Processes. After CTAB adsorption, a layer of positive charges was created on the surface of SWNTs. Therefore, polyanion PSS, positively charged ILs, and negatively charged GOx (at pH 8.2) could be assembled on the surface of SWNTs layer-by-layer based on electrostatic interaction, and the GOx−ILs−PSS−SWNTs/GC electrode was prepared. Those assembly processes were characterized by FTIR spectroscopy.

As shown in Figure 1a, for purified SWNTs, the characteristic vibration modes of the carbonyl group (~1640 cm^{-1}) and hydroxyl group (~3450 cm^{-1}) are obvious, demonstrating that SWNTs have been functionalized with carboxylic and carboxylate groups after treatment with acid.[47] The adsorption of CTAB on the surface of SWNTs results in the characteristic vibration of $-CH_3$ and $-CH_2-$ (~2850 and ~2920 cm^{-1}) in the IR spectrum (Figure 1b). After the assembly of PSS, several new peaks are found in Figure 1c. These peaks, which appear at ~1180, 1130, 1040, 1010, 830, 680, and 620 cm^{-1}, respectively, are the characteristic FTIR features of PSS,[48] indicating that PSS has been effectively assembled on the surface of SWNTs. From the FTIR of [bmim]−PSS−SWNTs depicted in Figure 1d, the characteristic vibration of the imidazole ring is obvious. These peaks appear at 3165, 1570, and 1465 cm^{-1}. The peak of 3120 cm^{-1} results from the stretching vibration of =C−H, and the peak at 1286 cm^{-1} is from the stretching vibration of C−N.[49] The peak of 1035 cm^{-1} corresponds to vibration of the B−F group.[49] Furthermore, the intensities of peaks of $-CH_3$ and $-CH_2-$ presented in Figure 1d become even stronger than those in Figure 1c due to the contribution of the $-CH_3$ and $-CH_2-$ group coming from [bmim]. The demonstration of amide I (1640 cm^{-1}) and amide II (1573 cm^{-1})[50,51] in the FTIR spectrum of GOx−[bmim]−PSS−SWNTs (Figure 1e) indicates that GOx has been successfully adsorbed on the SWNTs.

The FTIR results also indicate that GOx can be effectively assembled on the surface of SWNTs if [bmim] is replaced by [bmpyri] or [bmpyrro] (the FTIR spectra were not shown here). These results demonstrate that ILs and GOx can be effectively assembled on the surface of SWNTs layer-by-layer.

3.2. Effects of ILs on the Voltammetric Characteristics of FcA. In this investigation, FcA was used as a mediator for the GOx catalyzing the oxidation of glucose. The effects of the different ILs, which were immobilized on the surface of the electrode, on the voltammetric response of FcA were presented before the effects of these ILs on the enzymatic system were studied.

The cyclic voltammogram of FcA (0.5 mM) at the bare GC electrode is characterized by a couple of well-defined redox peaks with the anodic and cathodic peak potentials of 320 and 260 mV, respectively (Figure 2a). The redox peaks exhibit diffusion-controlled characteristics since both anodic and cathodic peak currents increase linearly with the square root of scan rates (not shown here), and moreover, the separation of anodic and cathodic peak potential (ΔE_p) is 60 mV, which is in agreement with that expected by theory. The cyclic voltammogram of FcA at the SWNTs/GC electrode also shows a couple of redox peaks (Figure 2e). However, the anodic and cathodic peak potentials shift to ~310 and ~265 mV (ΔE_p = 55 mV), respectively. The peak current at the SWNTs/GC electrode increases significantly due to the enhancement of the effective area of the electrode. After ILs were assembled on the surface of SWNTs, the peak currents of the FcA/FcA^+ couple decrease comparing those obtained at the SWNTs/GC electrode. The peak currents decrease following the IL sequence of [bmpyri] > [bmpyrro] > [bmim] (Figure 2b−d). However, the values of ΔE_p (54 ± 3 mV) and the formal potential $E^{0'}$ (290 ± 5 mV) remain almost unchangeable compared with those obtained at the SWNTs/GC electrode. Furthermore, peak currents measured at each electrode increase linearly with the square root of scan rates (not shown here). These results indicate that the reaction of FcA/FcA^+ is reversible and the electron transfer process is fast at the surface of each electrode even in the presence of ILs.

3.3. Effects of ILs on the Enzymatic Oxidation of Glucose. The kinetics of the catalytic oxidation of glucose by GOx employing FcA as a mediator has been characterized in our earlier work.[52] In the absence of the substrate, the mediator gives rise to a one-electron reversible cyclic voltammetric wave. It increases in height and progressively loses its chemical reversibility upon addition of glucose. The increase of the peak height

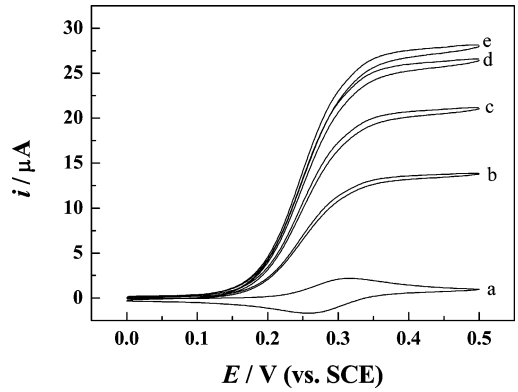

Figure 3. Electrocatalytic oxidation of 12 mM glucose at the GOx−[bmim]−PSS−SWNTs/GC (b), GOx−[bmpyrro]−PSS−SWNTs/GC (c), GOx−[bmpyri]−PSS−SWNTs/GC (d), and GOx−SWNTs/GC electrode (e) in 0.1 M PBS (pH 8.2) in the presence of 0.5 mM FcA as an electrochemical mediator. Curve (a) is the voltammetric response of the GOx−[bmim]−PSS−SWNTs/GC electrode in 0.1 M PBS (pH 8.2) containing 0.5 mM FcA. The scan rate was 10 mV/s.

is thus a measure of the kinetics of the overall catalytic reaction from which the pertinent rate constants could be derived. In this work, a similar approach is used for evaluating the effects of the ILs on the kinetics of the oxidation of glucose catalyzed by GOx, which is assembled on the surface of electrode via ILs and PSS. It is important to examine whether or not the assembled enzyme affects the electrochemical reversibility of the mediator at the electrode. Optimal efficiency of the catalysis is reached when the mediator couple remains electrochemistry reversible in the potential scan rate range of interest. The fulfillment of these conditions also simplifies the procedures of derivation of the catalysis kinetics from the experimental data.

A typical cyclic voltammogram of FcA (0.5 mM) at the GOx−[bmim]−PSS−SWNTs/GC electrode is presented in Figure 3a, which is characterized by a couple of redox peaks with the anodic and cathodic peak potential of 320 and 260 mV. The value of ΔE_p is 60 mV, and the peak currents increase linearly with the square root of scan rates, indicating FcA/FcA^+ undergoes a one-electron reversible redox reaction at the enzyme-assembled electrode surface. This conclusion is the same as that obtained in Section 3.2, suggesting that the presence of GOx on the surface of the electrode does not affect the electrochemical characteristics of the mediator. Similar results are obtained when [bmim] is replaced by [bmpyrro] or [bmpyri].

Upon the addition of glucose (12 mM), the anodic currents increase greatly at a potential of the oxidation of FcA, and a steady-state electrocatalytic plateau is observed (Figure 3b); in the meanwhile, the cathodic peak disappears completely. This is a typical characteristic for a steady-state electrocatalytic reaction. The catalytic process consists of the following sequence of reactions[53]

$$FcA \rightleftharpoons FcA^+ + e \quad (1)$$

$$GOx(FAD) + \text{glucose} \underset{k_{-1}}{\overset{k_1}{\rightleftharpoons}} GOx(FAD) \cdot \text{glucose} \quad (2)$$

$$GOx(FAD) \cdot \text{glucose} \xrightarrow{k_2} GOx(FADH_2) + \text{glucono-}\delta\text{-lactone} \quad (3)$$

$$GOx(FADH_2) + 2FcA^+ \xrightarrow{k_3} GOx(FAD) + 2FcA \quad (4)$$

where GOx(FAD) and $GOx(FADH_2)$ represent the oxidized and reduced form of GOx, respectively, and GOx(FAD)·glucose is the enzyme−substrate complex.

Figure 3c−e shows the electrocatalytic activity of the GOx−[bmpyrro]−PSS−SWNTs/GC (c), GOx−[bmpyri]−PSS−SWNTs/GC (d), and GOx−SWNTs/GC electrode (e), respectively, toward the oxidation of glucose (12 mM). At each electrode, a steady-state voltammetric response is reached. The catalytic current (i_{cat}) increases with the glucose concentration and levels off above 8 mM, showing a Michaelis−Menten characteristic (Figure 4). The limiting steady-state i_{cat} increases following the sequence of [bmim] < [bmpyrro] < [bmpyri] < SWNTs. Therefore, the concentration of substrate used in this work (12 mM) can confirm that the electrocatalytic reactions are proceeded under a substrate-saturated condition.

For the catalytic system of enzyme immobilized on the electrode and mediator dissolved in solution, the expression of i_{cat} obtained from the cyclic voltammograms can be given in eq 5[53]

$$\frac{1}{i_{cat}} = \frac{1}{2Fk_3\Gamma_E} \cdot \frac{1}{c_M} + \frac{1}{2F\Gamma_E}\left(\frac{1}{k_2} + \frac{1}{k_{red}} \cdot \frac{1}{c_G}\right) \quad (5)$$

where F is Faraday constant; Γ_E (in mol) is the total amount of GOx at the electrode surface; c_M is the concentration of the mediator in solution; and c_G is the concentration of substrate (glucose) in solution. The expression of k_{red} is $k_{red} = k_1k_2/(k_{-1} + k_2)$. The limiting steady current is dependent on the concentration of substrate and mediator and their associated kinetic constants. For each enzyme electrode, the magnitude of i_{cat}, checked at various glucose concentrations and amounts of enzyme on the electrode surface, was independent of the scan rate as predicted by the theory.

Once the amount of enzyme (Γ_E) on the electrode surface is known, the characteristic rate constant of the catalytic system can be derived from the cyclic voltammograms using the expression given in eq 5. The value of Γ_E on the electrode surface was determined spectrophotometrically from the change of the concentration of GOx in solution before and after adsorption on the surface of the electrode (see Experimental Section) and listed in Table 1. According to eq 5, at each glucose

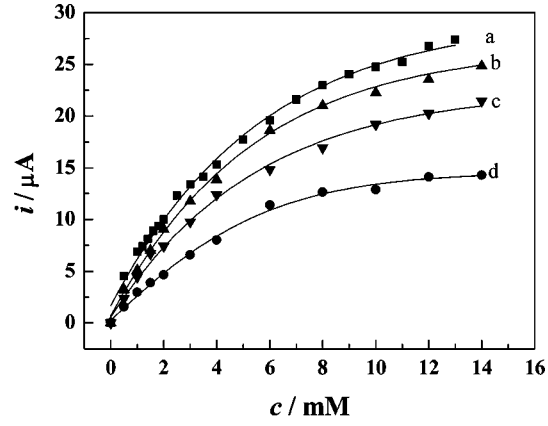

Figure 4. Dependence of the electrocatalytic current on the concentration of glucose obtained at the GOx−SWNTs/GC (a), GOx−[bmpyri]−PSS−SWNTs/GC (b), GOx−[bmpyrro]−PSS−SWNTs/GC (c), and GOx−[bmim]−PSS-SWNTs/GC electrode (d).

TABLE 1: Characteristic Rate Constants of Glucose Oxidation Catalyzed by GOx Immobilized on the Electrode Surface via ILs Using Dissolved FcA as Mediator[a]

electrodes	Γ_E (mol)	k_3 (M^{-1} s^{-1})	k_2 (s^{-1})	k_{red} (M^{-1} s^{-1})
GOx−SWNTs/GC	$(2.85 \pm 0.54) \times 10^{-13}$	$(3.78 \pm 0.51) \times 10^6$	717.5 ± 14.3	$(1.49 \pm 0.32) \times 10^4$
GOx−[bmpyri]−PSS−SWNTs/GC	$(3.46 \pm 0.46) \times 10^{-13}$	$(1.35 \pm 0.23) \times 10^5$	122.0 ± 11.3	$(8.84 \pm 0.43) \times 10^3$
GOx−[bmpyrro]−PSS−SWNTs/GC	$(3.62 \pm 0.38) \times 10^{-13}$	$(9.91 \pm 0.62) \times 10^4$	105.0 ± 9.1	$(7.03 \pm 0.35) \times 10^3$
GOx−[bmim]−PSS−SWNTs/GC	$(4.14 \pm 0.28) \times 10^{-13}$	$(6.81 \pm 0.56) \times 10^4$	91.9 ± 6.5	$(4.11 \pm 0.26) \times 10^3$
GOx−PDDA−PSS−SWNTs/GC	$(3.12 \pm 0.37) \times 10^{-13}$	$(3.42 \pm 0.48) \times 10^6$	723.1 ± 11.6	$(1.24 \pm 0.31) \times 10^4$
GOx dissolved in solution with O_2 as mediator[b]	-	-	750	1.1×10^4

[a] Each value is an average of three measurements at each electrode. [b] The value is from ref 54.

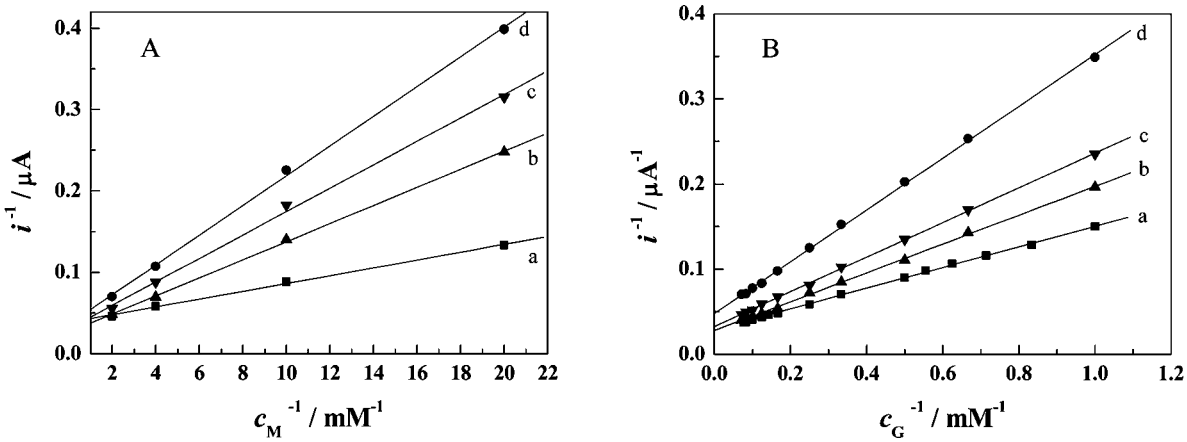

Figure 5. Double reciprocal plots of $1/i_{cat}$ against $1/c_M$ (A, at fixed concentration of glucose of 12 mM) and $1/i_{cat}$ against $1/c_G$ (B, at fixed concentration of mediator of 0.5 mM) for GOx−PSS−SWNTs/GC (a), GOx−[bmpyrro]−PSS−SWNTs/GC (b), GOx−[bmpyri]−PSS−SWNTs/GC (c), and GOx−[bmim]−PSS−SWNTs/GC electrode (d).

concentration, a straight line with a slope of $1/2Fk_3\Gamma_E$ can be obtained upon plotting $1/i_{cat}$ against $1/c_M$ (Figure 5A). By plotting $1/i_{cat}$ against $1/c_G$ at a fixed concentration of mediator (0.5 mM), another straight line with the slope and intercept of $1/2F\Gamma_E k_{red}$ and $1/2(1/Fk_3\Gamma_E c_M + 1/F\Gamma_E k_2)$, respectively, can also be obtained (Figure 5B). The characteristic kinetic constants of the enzymatic catalytic system (k_2, k_3, and k_{red}) can be derived from the values of these slopes and intercepts and are summarized in Table 1. For comparison, the values of k_{red} and k_2 for a homogeneous enzyme system (GOx was dissolved in solution) with O_2 as mediator are also listed in Table 1. It is indicated that the values of the characteristic rate constant obtained at the GOx−SWNTs/GC electrode are very close to those determined in the homogeneous system, indicating GOx immobilized on the surface of SWNTs is fully active. However, those characteristic rate constants obtained at each IL-containing enzyme electrode are lower than those obtained at the GOx−SWNTs/GC electrode; furthermore, the rate constants decrease following the sequence of SWNTs > [bmpyri] > [bmpyrro] > [bmim].

4. Discussion

There are several possible factors affecting the GOx enzymatic oxidation of glucose. As shown above and previously,[52] GOx immobilized on the surface of SWNTs is fully active and does not undergo denaturation. However, the presence of ILs on the surface of the electrode may lead the assembled GOx to denature since some organic reagents, including ILs, can change the native integrity of enzyme molecules and cause them to denature and lose the catalytic activity.

Usually, the enzymes' stability is mainly dependent on the type of the anion species of ILs.[34] ILs containing anions such as BF_4^-, PF_6^-, and Ntf_2^- (Ntf_2 = bis(trifluormethylsulfonyl)imide) render active enzymes, while NO_3^-, $CF_3CO_2^-$, and $CF_3SO_3^-$ inactivate enzymes.[30] CD spectra of GOx−[bmim]−PSS−SWNTs, GOx−[bmpyrro]−PSS−SWNTs, and GOx−[bmpyri]−PSS−SWNTs composites were recorded, respectively, to make sure GOx could still retain its native conformation after assembly on SWNTs via ILs. These composites were incubated in PBS (pH 8.2) for 2 h before CD spectra were recorded. The time scale is enough for each electrochemical measurement. The CD spectrum of GOx in solution was also recorded for comparison. The spectra in the far-UV region (200−250 nm) correspond to the peptide $n \rightarrow \pi^*$ electronic transition. The spectrum in this region is sensitive to the changes of the conformation of the enzyme.[55] The spectrum of GOx in solution in this region is characterized by two negative peaks at ~210 and ~218 nm, respectively (Figure 6A). These peaks almost remain invariable after the enzyme was assembled on the surface of SWNTs via ILs, indicating that the secondary structure and conformation of the immobilized GOx are essentially the same as that of the native one. Moreover, the spectra presented in Figure 6B show that the CD spectra of GOx−[bmim]−PSS−SWNTs (black), GOx−[bmpyrro]−PSS−SWNTs (red), and GOx−[bmpyri]−PSS−SWNTs (blue) are also the same as that of GOx dissolved in PBS (green). These results suggest that the microenvironment of the active site of GOx on the IL-containing electrode surface remains the same as that of the native one since no signals can be observed in this region for a denatured GOx due to the dissociation of FAD from the enzyme.[55]

The leakage of GOx molecules from the surface of the electrode may be a possible reason for the decrease of i_{cat}. The stability of the electrode responses, which can be taken as a measure of the persistency of the activity of the attached enzyme, was studied by cyclic voltammetry and was found to be remarkably good. The i_{cat} remains almost unchangeable even

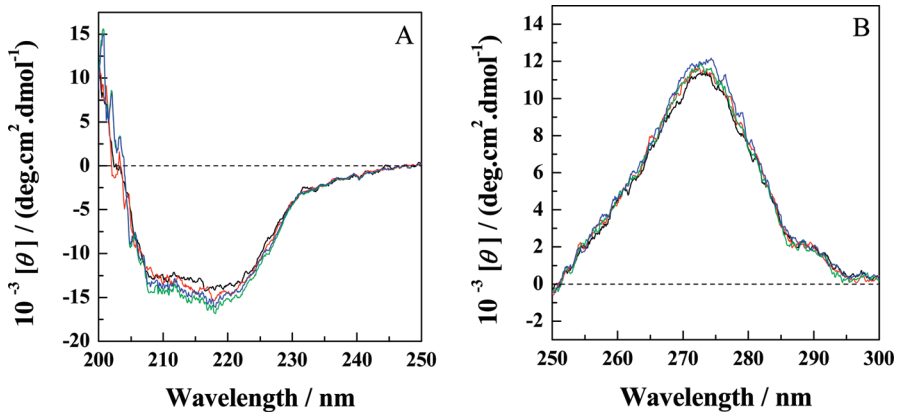

Figure 6. CD spectra of GOx−[bmim]−PSS−SWNTs (black), GOx−[bmpyrro]−PSS−SWNTs (red), and GOx−[bmpyri]−PSS−SWNTs (blue) incubated in PBS (0.1 M, pH 8.2) and pure GOx dissolved in PBS (1 mg/mL, green) in the far-UV (A) and near-UV (B) region.

after the electrode is continuously scanned for 50 cycles (at scan rate of 10 mV/s). If the enzyme electrodes were stored in PBS buffer, the electrode response has ~0.2% decay per day, indicating the storage stability is good. These characteristics were not affected by the types of ILs. These results indicate that the stability of the GOx is high, and the GOx molecules do not leak from the surface of the electrode even in the presence of ILs. Otherwise, the i_{cat} should gradually decrease with continuous scanning. This conclusion is in good agreement with that obtained from CD measurements.

The coverage of the enzyme on the surface of the electrode may also become a possible factor affecting the characteristic rate constants of the catalytic system. The total amount of enzyme presented at the electrode surface (Γ_E) was varied by changing the concentration of the enzyme in the solution where the electrode was incubated and the duration of its exposure to the solution. As shown in the Experimental Section, this work optimized these conditions. It was observed that, upon increasing one or the other of these factors, the magnitude of i_{cat} reached a limiting value indicating that the electrode surface then became saturated in enzyme. Therefore, those factors, for which the saturated amount of the enzyme on the electrode surface can be reached, were selected to fabricate an enzyme electrode.

As presented in Table 1, the total amount of enzyme at saturation is $(2.85 \pm 0.54) \times 10^{-13}$, $(3.46 \pm 0.46) \times 10^{-13}$, $(3.62 \pm 0.38) \times 10^{-13}$, and $(4.14 \pm 0.28) \times 10^{-13}$ mol for the GOx−SWNTs/GC, GOx−[bmpyri]−PSS−SWNTs/GC, GOx−[bmpyrro]−PSS−SWNTs/GC, and GOx−[bmim]−PSS−SWNTs/GC electrode, respectively. These values correspond to $(2.38 \pm 0.45) \times 10^{-12}$, $(2.16 \pm 0.29) \times 10^{-12}$, $(2.01 \pm 0.21) \times 10^{-12}$, and $(1.97 \pm 0.13) \times 10^{-12}$ mol cm^{-2}, respectively, by considering the effective surface of each electrode. The molecule of GOx is a compact ellipsoid whose size is 5.2 nm × 6.0 nm × 7.7 nm.[56,57] However, the Stokes radius (4.3 nm) is a reasonable value usually used for estimating the occupation area of each GOx molecule (~58 nm^2) since each molecule may be assembled in various orientations and the assembly process may proceed randomly.[58] Therefore, the superficial concentration of the enzyme corresponding to the saturation monolayer should be $\sim 2.86 \times 10^{-12}$ mol cm^{-2}. Although the above size and surface area estimates are certainly approximate, one can conclude that the surface of each electrode is covered by a monolayer of close-packed enzyme units. Thus, the coverage of GOx at each electrode cannot be a possible factor inducing the decrease of the characteristic rate constants as presented in Table 1.

Comparing with the GOx−SWNTs/GC electrode, a layer of polyanion PSS is presented at each GOx−IL−PSS−SWNTs/GC electrode as illustrated in the electrode fabrication process (Scheme 1). This layer of PSS may increase the distance between the substrate GC surface and redox species and thus block the electron transfer leading to the decrease of the rate constants of the catalytic system. However, the results depicted in Figure 2 and Figure 3a demonstrated that FcA/FcA$^+$ couple underwent a one-electron reversible redox reaction even with the presence of PSS and GOx at the surface of the electrode. Therefore, the layer of PSS on the IL-containing electrode surface does not obstruct the electron transfer of the redox couple of FcA/FcA$^+$ and is not a factor of causing the decrease of rate constants as shown in Table 1.

To further verify this conclusion, ILs were replaced by PDDA, a positively charged polyelectrolyte, to assemble GOx on the electrode surface forming the GOx−PDDA−PSS−SWNTs/GC electrode (steps d and e, Scheme 1). The electrocatalytic oxidation of glucose at the electrode was studied, and the characteristic rate constants of this catalytic system were determined using the same approach as that for the GOx−SWNTs/GC and GOx−IL−PSS−SWNTs/GC electrodes. The rate constants obtained at the electrode are also shown in Table 1, which indicates that the values of the characteristic rate constants obtained at the electrode are similar to those derived at the GOx−SWNTs/GC electrode. However, they are higher than those derived from the GOx−IL−PSS−SWNTs/GC electrodes. These results further demonstrate that the layer of PSS on the electrode surface cannot be a possible reason for causing the decrease of characteristic rate constants of the catalytic system.

After eliminating the above possible factors, we next consider the effects of IL nature on the enzymatic oxidation of glucose. To explain the effects better, the electrical properties of the [bmpyri], [bmpyrro], and [bmim] on SWNTs were investigated based on the quantum chemistry method. All the compounds have been fully optimized using the DFT/B3LYP method with the 6-31G* basis set and characterized by the calculations of vibrational frequencies at the same level. The conductor-like polarizable continuum model (CPCM)[59] was employed in these calculations, and the dielectric constant of water at 298.15 K (78.4) was used to simulate the aqueous environment. All the theoretical calculations are carried out with the use of the GAUSSIAN 03 program package[60] with the default convergence criteria, and the frontier molecular orbital surfaces are visualized using Gauss View.[61] To simplify the calculation, we only considered the interaction between the SWNTs and the IL molecules.

The optimized molecule structures and atom-numbering of [bmpyri], [bmpyrro], and [bmim] are depicted in Figure 7.

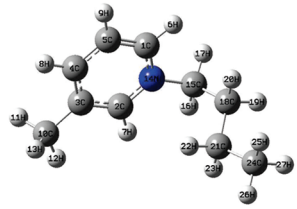

[bmpyri]

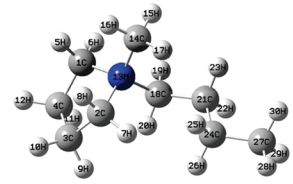

[bmpyrro]

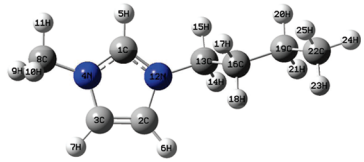

[bmim]

Figure 7. Optimized molecule structure and atom-numbering of [bmpyri], [bmpyrro], and [bmim].

Structures along with the Mulliken atomic charges for the non-hydrogen atoms and partial selected hydrogen atoms with high charge density for the three molecules in water are presented in Figure 8. The optimized results reveal that the pyridine ring in [bmpyri] and the imidazole ring in [bmim] are conjugated and planar, while the pyrrolidine ring in [bmpyrro] is unconjugated and is also not planar. The butyl group is almost vertical to the heterocycle with a dihedral angle of −104.9, −82.9, and −79.3° for [bmpyri], [bmpyrro], and [bmim], respectively. This configuration of the butyl group favors the assembly of the molecules at the surface of SWNTs since the steric exclusion of the butyl group can be significantly decreased.

Localization of frontier molecular orbitals and the charge distributions were employed to analyze interactions between SWNTs and the assembled species and to explain the effects of the assembled species on the electrical properties of SWNTs. The highest occupied molecular orbital (HOMO) and the lowest unoccupied molecular orbital (LUMO) surfaces for [bmpyri], [bmpyrro], and [bmim] are given in Figure 9. HOMO location mostly distributes in the whole molecule for [bmpyri] and [bmim], while HOMO location only distributes in the butyl in [bmpyrro]. However, LUMO location in the three molecules mostly distributes in the vicinity of the nitrogen atom, namely, the pyridine, imidazole, and pyrrolidine ring, respectively. The results indicate that the interaction between SWNTs and the assembled species mainly takes place via the nitrogen atom, and consequently, the charge transfer between SWNTs and the ILs occurs mainly at nitrogen.

It was reported that the charge transfer from SWNTs to absorbed nitrogen or oxygen atom would enhance conductance of SWNTs, while the charge transfer from the absorbed nitrogen or oxygen atom to SWNTs would lead to the decrease of the conductance of SWNTs.[62] From the calculated results, one can find that the nitrogen atom in the [bmpyri] molecule carries 0.237 au positive charge, while that in [bmpyrro] and [bmim] molecules carries −0.549 and −0.122 (−0.084) au negative charge, respectively. These results suggest that the charge

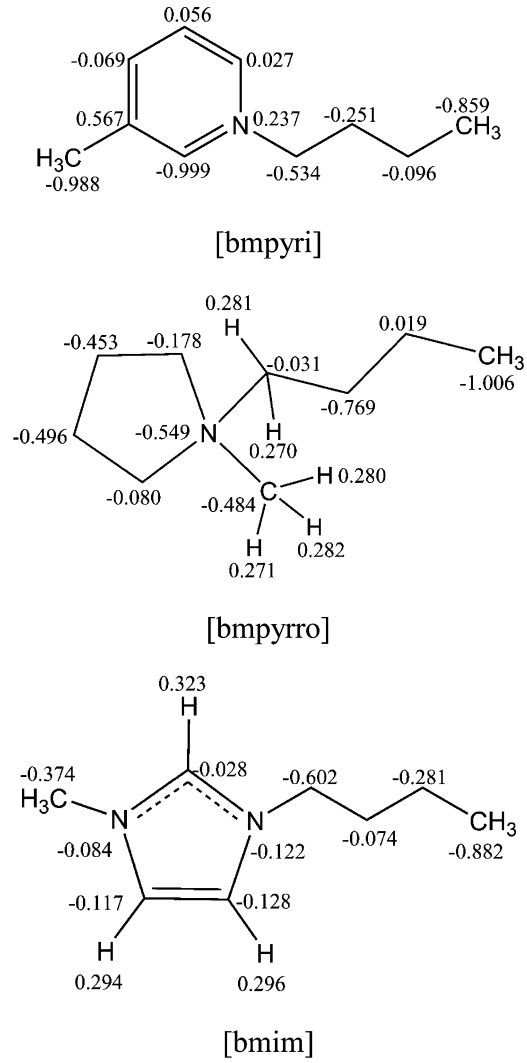

Figure 8. Mulliken atomic charge of all the non-hydrogen atoms and partial selected hydrogen atoms for [bmpyri], [bmpyrro], and [bmim] at the ground state in water.

transfer direction is from SWNTs to [bmpyri] in the case of [bmpyri]−SWNTs and the charge transfer is from [bmpyrro] (or [bmim]) to SWNTs in the case of [bmpyrro]−SWNTs and [bmim]−SWNTs. Therefore, the conductance of [bmpyri]−SWNTs would be higher than those for [bmpyrro]−SWNTs and [bmim]−SWNTs. The changes in conductive characteristics of SWNTs after assembly of different ILs will affect the electrocatalytic activity of GOx−IL−PSS−SWNT/GC electrodes and result in the change of the characteristic rate constants of glucose oxidation as shown in Table 1.

The value of Δq, which is defined as the difference between the highest positive and negative net charge, of [bmpyri], [bmpyrro], and [bmim] is also an important factor affecting the electrical transfer properties of [bmpyri]−SWNTs, [bmpyrro]−SWNTs, and [bmim]−SWNTs. A high value of Δq will be of benefit to electrical transfer and results in the high electrocatalytic activity. From Figure 8, the value of Δq for [bmpyri], [bmpyrro], and [bmim] is 1.566, 1.288, and 1.205, respectively. These results indicate that the electrocatalytic activity of GOx−IL−PSS−SWNT/GC electrodes will decrease in the order of [bmpyri], [bmpyrro], and [bmim], which is in good agreement with the results depicted in Table 1. Therefore, the nature of ILs significantly affects the electrocatalytic activity of GOx−IL−

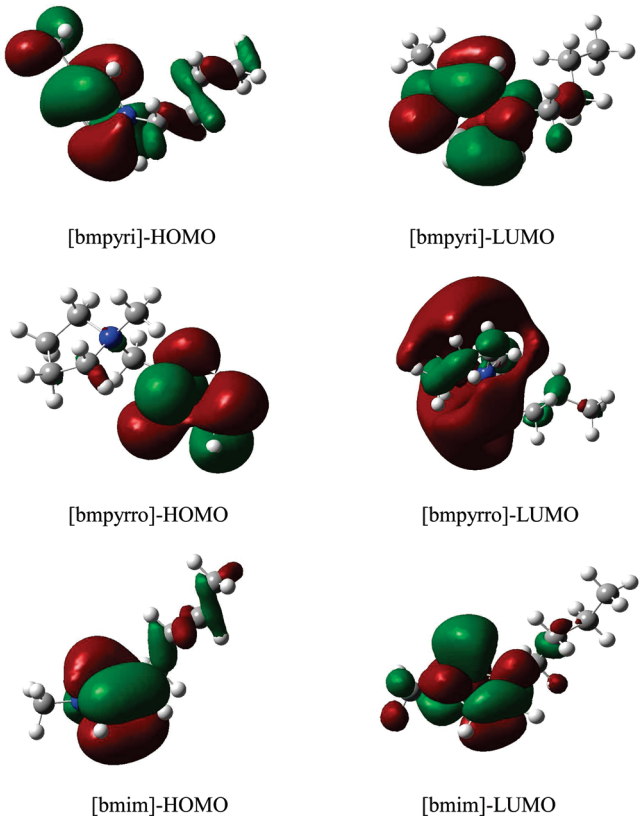

Figure 9. Highest occupied molecular orbital (HOMO) and the lowest unoccupied molecular orbital (LUMO) surfaces for [bmpyri], [bmpyrro], and [bmim].

PSS−SWNT/GC electrodes toward the oxidation of glucose and is a key factor governing the electrocatalytic activity of the electrode.

5. Conclusions

The effects of ILs on the electrocatalytic activty of GOx toward the oxidation of glucose have been studied with the use of cyclic voltammetry and the theoretical calculation method. Three types of ILs of [bmpyri]BF_4, [bmpyrro]BF_4, and [bmim]BF_4 were selected to study the effects of different types of ILs on the catalytic system. The characteristic kinetic constants for the enzymatic reaction were evaluated from the cyclic voltammograms, indicating that the values of these rate constants decrease following the sequence of SWNTs > [bmpyri] > [bmpyrro] > [bmim]. The results of theoretical calculations showed that the presence of IL on the surface of SWNTs can significantly affect the electrical transfer properties of the nanotube and lead to the decrease of the electrocatalytic activity of the GOx. Therefore, this work concludes that the nature of ILs is a key factor of affecting the electrocatalytic activity of GOx−IL−PSS−SWNT/GC electrodes toward the oxidation of glucose.

Acknowledgment. This work is supported by the National Natural Science Foundation of China (20673057, 20773067, 20833006, and 20905036), the Program for New Century Excellent Talents in University (NET-06-0508), and the Foundation of the Jiangsu Education Committee (09KJA150061).

References and Notes

(1) Welton, T. *Chem. Rev.* **1999**, *99*, 2071.
(2) Plechkova, N. V.; Seddon, K. R. *Chem. Soc. Rev.* **2008**, *37*, 123.
(3) Ohno, H. *Electrochemical Aspects of Ionic Liquids*; John Wiley & Sons: Hoboken, NJ, 2005.
(4) Handy, S. T. *Chem.−Eur. J.* **2003**, *9*, 2938.
(5) Zhang, S. J.; Sun, N.; He, X. Z.; Lu, X. M.; Zhang, X. P. *J. Phys. Chem. Ref. Data* **2006**, *35*, 1475.
(6) Zerth, H. M.; Leonard, N. M.; Mohan, R. S. *Org. Lett.* **2003**, *5*, 55.
(7) Chun, S.; Dzyuba, S. V.; Bartsch, R. A. *Anal. Chem.* **2001**, *73*, 3737.
(8) Rumbau, V.; Marcilla, R.; Ochoteco, E.; Pomposo, J. A.; Mecerreyes, D. *Macromolecules* **2006**, *39*, 8547.
(9) Anderson, J. L.; Armstrong, D. W. *Anal. Chem.* **2005**, *77*, 6453.
(10) Dash, P.; Scott, R. W. *Chem. Commun.* **2009**, 812.
(11) (a) Belieres, J. P.; Gervasio, D.; Angell, C. A. *Chem. Commun.* **2006**, *46*, 4799. (b) Pomfret, M. B.; Brown, D. J.; Epshteyn, A.; Purdy, A. P.; Owrutsky, J. C. *Chem. Mater.* **2008**, *20*, 5945.
(12) Zhao, C.; Burrell, G.; Torriero, A. A. J.; Separovic, F.; Dunlop, N. F.; MacFarlane, D. R.; Bond, A. M. *J. Phys. Chem. B* **2008**, *112*, 6923.
(13) (a) Zhao, F.; Wu, X.; Wang, M.; Liu, Y.; Gao, L.; Dong, S. *Anal. Chem.* **2004**, *76*, 4960. (b) Nishi, N.; Imakura, S.; Kakiuchi, T. *Anal. Chem.* **2006**, *78*, 2726.
(14) Yu, P.; Lin, Y.; Xiang, L.; Su, L.; Zhang, J.; Mao, L. *Langmuir* **2005**, *21*, 9000.
(15) Kachoosangi, R. T.; Musameh, M. M.; Abu-Yousef, I.; Yousef, J. M.; Kanan, S. M.; Xiao, L.; Davies, S. G.; Russell, A.; Compton, R. G. *Anal. Chem.* **2009**, *81*, 435.
(16) Maleki, N.; Safavi, A.; Tajabadi, F. *Anal. Chem.* **2006**, *78*, 3820.
(17) (a) Moustafa, E. M.; Zein El Abedin, S.; Shkurankov, A.; Zschippang, E.; Saad, A. Y.; Bund, A.; Endres, F. *J. Phys. Chem. B* **2007**, *111*, 4693. (b) Mann, O.; Freyland, W. *J. Phys. Chem. C* **2007**, *111*, 9832. (c) Wang, Y.; Yang, H. *J. Am. Chem. Soc.* **2005**, *127*, 5316. (d) Batra, D.; Seifert, S.; Varela, L. M.; Liu, A. C. Y.; Firestone, M. A. *Adv. Funct. Mater.* **2007**, *17*, 1279. (e) Endres, F. *ChemPhysChem* **2002**, *3*, 144. (f) Imanishi, A.; Tamura, M.; Kuwabata, S. *Chem. Commun.* **2009**, 1775.
(18) Matsumiya, M.; Terazono, M.; Tokuraku, K. *Electrochim. Acta* **2006**, *51*, 1178.
(19) Silverster, D. S.; Compton, R. G. *Z. Phys. Chem.* **2006**, *220*, 1247.
(20) Lu, X.; Zhang, Q.; Zhang, L.; Li, J. *Electrochem. Commun.* **2006**, *8*, 874.
(21) Lu, X.; Hu, J.; Yao, X.; Wang, Z.; Li, J. *Biomacromolecules* **2006**, *7*, 975.
(22) Shimojo, K.; Goto, M. *Anal. Chem.* **2004**, *76*, 5039.
(23) Ding, S.-F.; Xu, M.-Q.; Zhao, G.-C.; Wei, X.-W. *Electrochem. Commun.* **2007**, *9*, 216.
(24) Wang, S.-F.; Chen, T.; Zhang, Z.-L.; Pang, D.-W.; Wong, K.-Y. *Electrochem. Commun.* **2007**, *9*, 1709.
(25) Compton, D. L.; Laszlo, J. A. *J. Electroanal. Chem.* **2003**, *553*, 187.
(26) Li, J.; Fan, C.; Xiao, F.; Yan, R.; Fan, S.; Zhao, F.; Zeng, B. *Electrochim. Acta* **2007**, *52*, 6178.
(27) Zhang, Y.; Shen, Y.; Han, D.; Wang, Z.; Song, J.; Li, F.; Niu, L. *Biosens. Bioelectron.* **2007**, *23*, 438.
(28) van Rantwijk, F.; Sheldon, R. A. *Chem. Rev.* **2007**, *107*, 2757.
(29) Moniruzzaman, M.; Kamiya, N.; Goto, M. *Langmuir* **2009**, *25*, 977.
(30) Micaêlo, N. M.; Soares, C. M. *J. Phys. Chem. B* **2008**, *112*, 2566.
(31) Imabayashi, S.; Ishii, K.; Watanabe, M. *Electrochem. Commun.* **2006**, *8*, 45.
(32) Yang, Z.; Pan, W. *Enzyme Microb. Technol.* **2005**, *37*, 19.
(33) Park, S.; Kazlauska, R. J. *Curr. Opin. Biotechnol.* **2003**, *14*, 432.
(34) Kaar, J. L.; Jesionowski, A. M.; Berberich, J. A.; Moulton, R.; Russel, A. J. *J. Am. Chem. Soc.* **2003**, *125*, 4125.
(35) Lau, R. M.; Sorgedrager, M. J.; Carrea, G.; van Rantwijk, F.; Secundo, F.; Sheldon, R. A. *Green Chem.* **2004**, *6*, 483.
(36) de Diego, T.; Lozano, P.; Gmouh, S.; Vaultier, M.; Iborra, J. L. *Biotechnol. Bioeng.* **2004**, *88*, 916.
(37) Ulbert, O.; Belafi-Bako, K.; Tonova, K.; Gubicza, L. *Biocatal. Biotransform.* **2005**, *23*, 177.
(38) Zhang, J.; Lei, J. P.; Liu, Y. Y.; Zhao, J. W.; Ju, H. X. *Biosens. Bioelectron.* **2009**, *24*, 1858.
(39) Tu, W. W.; Lei, J. P.; Ju, H. X. *Chem.−Eur. J.* **2009**, *15*, 779.
(40) Du, P.; Liu, S.; Wu, P.; Cai, C.-X. *Electrochim. Acta* **2007**, *52*, 6534.
(41) Wu, X.; Du, P.; Wu, P.; Cai, C.-X. *Electrochim. Acta* **2008**, *54*, 738.
(42) Du, P.; Zhou, B.; Cai, C.-X. *J. Electroanal. Chem.* **2008**, *614*, 149.
(43) Wang, Z.; Liu, S.; Wu, P.; Cai, C.-X. *Anal. Chem.* **2009**, *81*, 1638.
(44) Tohji, K.; Goto, T.; Takahashi, H.; Shinoda, Y.; Shimizu, N.; Jeyadevan, B.; Matsuoka, I. *Nature* **1996**, *383*, 679.
(45) Kim, K. K.; Fravel, D. R.; Papavizas, G. C. *Can. J. Microbiol.* **1990**, *36*, 760.
(46) Swoboda, B. E. P.; Massey, V. *J. Biol. Chem.* **1965**, *240*, 2209.

(47) Lim, J. L.; Yun, W. S.; Yoon, M. H.; Lee, S. K.; Kim, S. K. *Synth. Met.* **2003**, *139*, 521.
(48) Yang, J. C.; Jablonsky, M. J.; Mays, J. W. *Polymer* **2002**, *43*, 5125.
(49) Chowdhury, A.; Thynell, S. T. *Thermochim. Acta* **2006**, *443*, 159.
(50) Niwa, K.; Furukawa, M.; Niki, K. *J. Electroanal. Chem.* **1988**, *245*, 275.
(51) Irace, G.; Bismuto, E.; Savy, F.; Colonna, G. *Arch. Biochem. Biophys.* **1986**, *244*, 459.
(52) Cai, C.-X.; Chen, J. *Anal. Biochem.* **2004**, *332*, 75.
(53) Bourdillon, C.; Demaille, C.; Gueris, J.; Moiroux, J.; Savéant, J.-M. *J. Am. Chem. Soc.* **1993**, *115*, 12264.
(54) Weibel, M. K.; Bright, H. *J. Biol. Chem.* **1971**, *246*, 2734.
(55) Zoldák, G.; Zubrik, A.; Musatov, A.; Stupák, M.; Sedlák, E. *J. Biol. Chem.* **2004**, *279*, 47601.
(56) Hecht, H. J.; Kalisz, H. M.; Handle, J.; Schmid, R. D.; Schomburg, D. *J. Mol. Biol.* **1993**, *229*, 153.
(57) Wu, S.; Wu, J.; Liu, Y. Y.; Ju, H. X. *Chem. Mater.* **2008**, *20*, 1397.
(58) Szucs, A.; Hitchens, G. D.; Bockris, J. O'M. *J. Electrochem. Soc.* **1989**, *136*, 3748.
(59) Barone, V.; Cossi, M. *J. Phys. Chem.* **1998**, *102*, 1995.
(60) Frisch, M. J.; Trucks, G. W.; Schlegel, H. B.; Scuseria, G. E.; Robb, M. A.; Cheeseman, J. R. ; Montgomery, J. A., Jr.; Vreven, T.; Kudin, K. N.; Burant, J. C.; Millam, J. M.; Iyengar, S. S.; Tomasi, J.; Barone, V.; Mennucci, B.; Cossi, M.; Scalmani, G.; Rega, N.; Petersson, G. A.; Nakatsuji, H.; Hada, M.; Ehara, M.; Toyota, K.; Fukuda, R.; Hasegawa, J.; Ishida, M.; Nakajima, T.; Honda, Y.; Kitao, O.; Nakai, H.; Klene, M.; Li, X.; Knox, J. E.; Hratchian, H. P.; Cross, J. B.; Bakken, V.; Adamo, C.; Jaramillo, J.; Gomperts, R.; Stratmann, R. E.; Yazyev, O.; Austin, A. J.; Cammi, R.; Pomelli, C.; Ochterski, J. W.; Ayala, P. Y.; Morokuma, K.; Voth, G. A.; Salvador, P.; Dannenberg, J. J.; Zakrzewski, V. G.; Dapprich, S.; Daniels, A. D.; Strain, M. C.; Farkas, O.; Malick, D. K.; Rabuck, A. D.; Raghavachari, K.; Foresman, J. B.; Ortiz, J. V.; Cui, Q.; Baboul, A. G.; Clifford, S.; Cioslowski, J.; Stefanov, B. B.; Liu, G.; Liashenko, A.; Piskorz, P.; Komaromi, I.; Martin, R. L.; Fox, D. J.; Keith, T.; Al.Laham, M. A.; Peng, C. Y.; Nanayakkara, A.; Challacombe, M.; Gill, P. M. W.; Johnson, B.; Chen, W.; Wong, M. W.; Gonzalez, C.; Pople, J. A. *Gaussian 03*, Revision B.03; Gaussian, Inc.: Pittsburgh, PA, 2004.
(61) *Gauss View*, Version 3.0; Gaussian Inc.: Pittsburgh, PA, 2003.
(62) Kong, J.; Franklin, N. R.; Zhou, C.; Chapline, M. G.; Peng, S.; Cho, K.; Dai, H. *Science* **2000**, *287*, 622.

JP905632K